



Syntheses and electrochemistry of $(p\text{-XC}_6\text{H}_4\text{O})_6\text{W}$ (1-X , $\text{X} = \text{H}, \text{CH}_3, \text{OCH}_3, \text{Cl}, \text{Br}, \text{OH}, \text{OCH}_2\text{Ph}$) and $(p\text{-XC}_6\text{H}_4\text{O})_5\text{W}(\text{OC}_6\text{H}_4\text{OH})$ ($\text{X} = \text{H}, \text{CH}_3, \text{OCH}_3, \text{Cl}, \text{Br}$): an approach to electrocatalytic CH bond activation

Orson L. Sydora, Jonas I. Goldsmith, Thomas P. Vaid, Abigail E. Miller, Peter T. Wolczanski*, Hector D. Abruña

Department of Chemistry and Chemical Biology, Baker Laboratory, Cornell University Ithaca, NY 14853, USA

Received 21 May 2004; accepted 25 August 2004

Available online 25 September 2004

Abstract

Alcoholysis of $\text{W}(\text{OMe})_6$ afforded $(p\text{-PhCH}_2\text{OC}_6\text{H}_4\text{O})_6\text{W}$ ($1\text{-OCH}_2\text{Ph}$), which could be hydrogenated (10% Pd/C, 1 atm H_2) to prepare $(p\text{-HOC}_6\text{H}_4\text{O})_6\text{W}$ (1-OH). Related alcoholyses of WCl_6 with $\text{HOC}_6\text{H}_4\text{-}p\text{-X}$ provided the hexaphenoxides $(p\text{-XC}_6\text{H}_4\text{O})_6\text{W}$ (1-X , $\text{X} = \text{H}, \text{CH}_3, \text{OCH}_3, \text{Cl}, \text{Br}$) through minor modifications of literature procedures. Acid catalyzed treatment of 1-X with $p\text{-HOC}_6\text{H}_4\text{OCH}_2\text{Ph}$ provided a mixture of substitution products $(p\text{-XC}_6\text{H}_4\text{O})_{6-x}\text{W}(\text{OC}_6\text{H}_4\text{OCH}_2\text{Ph})_x$ ($x = 1$, 5-X) that could be hydrogenated (10% Pd/C, 1 atm H_2) to a mixture of hydroxylated products. Chromatography permitted isolation of $(p\text{-XC}_6\text{H}_4\text{O})_5\text{W}(\text{OC}_6\text{H}_4\text{OH})$ (6-X , $\text{X} = \text{H}, 19\%$; Me, 29%; $\text{OCH}_3, 19\%$; Cl, 12%; Br, 11%) in modest yields. Hexaphenoxides 1-X and 6-X manifested two electrochemical reduction waves whose positions were a function of *para*-substituent. When oxidized, 6-X and 1-OH were proposed to behave as $\text{W}(\text{V})$ quinone mimics, albeit at potentials capable of oxidizing hydrocarbons as shown via a thermochemical cycle. If the proposed transients $(p\text{-XC}_6\text{H}_4\text{O})_5\text{W}(\text{OC}_6\text{H}_4\text{O})$ (7-X) were generated, degradation was apparently competitive with CH bond activation. The structure of oligomeric $\{\text{K}[(p\text{-ClC}_6\text{H}_4\text{O})_6\text{W}]\}_\infty$ (8-Cl) is addressed, and comments on the nature of radical CH bond activation in this and related systems are presented.

© 2004 Elsevier Ltd. All rights reserved.

1. Introduction

The direct conversion of alkanes to functionalized products is a tremendously important, yet very difficult chemical transformation facing the organotransition metal community. The stoichiometric activation of carbon–hydrogen bonds has now been achieved in numerous systems [1,2], but the capability to catalyze this reaction concomitant with oxidation of the substrate has rarely been successfully realized [3–14]. To date,

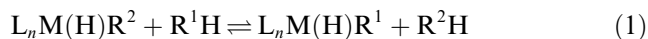
only autoxidation processes mediated by cobalt and manganese have been shown to be commercially viable, and these are rather specialized applications (e.g., $\text{C}_6\text{H}_{12} \rightarrow \text{HO}_2\text{C}(\text{CH}_2)_4\text{CO}_2\text{H}$, $\text{tBuH} \rightarrow \text{tBuOOH}$, $p\text{-MeC}_6\text{H}_4\text{Me} \rightarrow p\text{-HO}_2\text{CC}_6\text{H}_4\text{CO}_2\text{H}$, etc.) that have a minimum of selectivity issues [15,16].

Organometallic approaches to C–H bond activation have generated at least one major conceptual advance. In stark contrast to known free radical chemistry, organometallic systems tend to oxidatively or otherwise add stronger CH bonds selectively over weaker. While some have argued for steric interpretations of these events, it seems clear that this CH bond activation selectivity stems from the greater $D(\text{M-R})$ derived from

* Corresponding author. Tel.: +1 607 255 7220; fax: +1 607 255 4137.

E-mail address: ptw2@cornell.edu (P.T. Wolczanski).

activation of the stronger bond. For example, in Eqs. (1) and (2), if $\Delta G_{\text{rxn}}^0 \sim \Delta H_{\text{rxn}}^0$ and the bonds in $L_n\text{MH}$ (Eq. (1)) or $L_n\text{MXH}$ (Eq. (2)) are relatively unaffected by R^1 versus R^2 , then $\Delta H_{\text{rxn}}^0 = \{D(\text{M}-\text{R}^2) - D(\text{MR}^1)\} + \{D(\text{R}^1\text{H}) - D(\text{R}^2\text{H})\}$. As long as the differences in $D(\text{M}-\text{R}^n)$ are greater than the differences in $D(\text{H}-\text{R}^n)$ (i.e., $\Delta D(\text{M}-\text{R}^n)/\Delta D(\text{H}-\text{R}^n) > 1$), selectivities opposite to that of free radical activations prevail: $\text{sp-CH} > \text{Ar-H} \geq \text{sp}^2\text{-CH}$, including ${}^{\text{c}}\text{PrH} > \text{MeH} > 1^\circ\text{sp}^3\text{-CH} > 2^\circ\text{sp}^3\text{-CH} > 3^\circ\text{sp}^3\text{-CH}$, with benzylic and allylic CH bonds often modest exceptions [17–19]. It seems clear that when Green [20] discovered the proclivity of transiently generated tungstenocene to activate arene CH bonds (Eq. (3)), it was this selectivity that was first being witnessed. In most systems involving direct oxidative addition of carbon–hydrogen bonds, this selectivity is modest because binding of R^nH precedes C–H bond cleavage [17,18]. In cases where the actual CH activation is rate-determining [20], there is considerable optimism that problems such as methane to methanol and acetic acid [6,7], and terminal versus internal $\text{sp}^3\text{-CH}$ activation and functionalization of acyclic alkanes will ultimately be solved [13,14].



Concerted types of C–H bond activations have been separated into various classes such as σ -bond metathesis, oxidative addition, 1,2-RH-addition and electrophilic activation [1]. While each represents a particular class of reactions, it is clear that electrophilic attack at the C–H bond, whether in a binding or cleavage event, is a common thread among these paths. Free radical and metalaradical (e.g., $L_n\text{M} + \text{RH} \rightarrow L_n\text{MH} + \text{R}^\cdot$; $L_n\text{MX} + \text{RH} \rightarrow L_n\text{MXH} + \text{R}^\cdot$, etc.) mechanisms for alkane activation may also yield some control, provided selectivity is built into the metal framework as in nature, or the precise $D(\text{R}^n\text{H})$ limits of activation can be controlled and utilized.

Many bioinorganic systems, most notably methane monooxygenase [21], cytochrome P-450 [22], and related oxidases [23–25], have been examined in the context of CH bond activation. Some exciting recent results have been obtained by Que, who has employed the tetramethylcyclam ligand in stabilizing an Fe(IV) oxo complex [26], and has expanded his ligand arsenal to pentadentate ligands whose ligated $\text{Fe}^{\text{IV}}=\text{O}$ groups are capable of hydroxylating cyclohexane and substrates containing weaker CH bonds [27]. Note that the metal functionality (MX) that reacts with RH need not be an oxo or multiple-bonded entity, but the transfer of a hydrogen atom to MX must satisfy certain thermodynamic requirements for it to occur with reasonable facility.

The thermodynamic feasibility of CH bond activation can be predicted with a thermochemical cycle devised by Parker and Tilset that use physically measurable parameters (i.e., E_{ox}^0 , $\text{p}K_a$, C) to determine the homolytic bond dissociation energies (BDEs) of X–H species [28]. Fig. 1 illustrates such a cycle in which CH bond activation can be done electrocatalytically [4] provided the reactive intermediate, $L_n\text{MX}$, is generated at a potential positive enough to abstract a hydrogen atom. The sequence gives the BDE (sol) of the X–H bond, which constitutes a reasonable thermodynamic limit of the CH bond that can be broken through H atom abstraction by $L_n\text{MX}$. Mayer [29] has used similar cycles in rationalizing oxidations of permanganate [30] and MMO mimics [31]. Herein is explored the generation of a W^{VI} (semiquinone)/ W^{V} (quinone) as a functionality that should be capable of the desired abstraction. Unfortunately, this specific system failed to generate products of CH activation, but a closer look at its features yields some surprises regarding CH bond activations by $L_n\text{MX}$.

2. Results

2.1. Syntheses

2.1.1. (*p*-PhCH₂OC₆H₄O)₆W (1-OCH₂Ph) and (*p*-HO-C₆H₄O)₆W (1-OH)

In an earlier project designed with the synthesis of inorganic dendrimers, the robust character of the hexaaryloxid tungsten coordination environment was exploited as shown in Scheme 1. Treatment of $\text{W}(\text{OMe})_6$, prepared from $\text{W}(\text{OMe})_4\text{Cl}_2$, MeOH and NEt_3 [32], with *p*-HOC₆H₄OCH₂Ph in toluene for 24 h

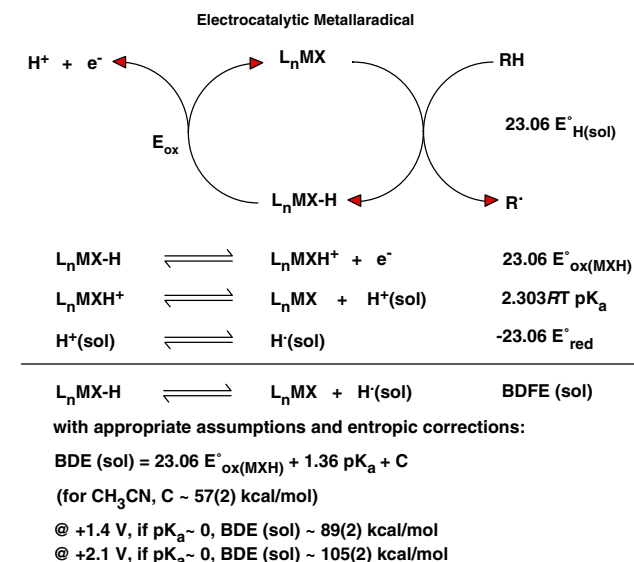


Fig. 1. Electrocatalytic metallaradical.

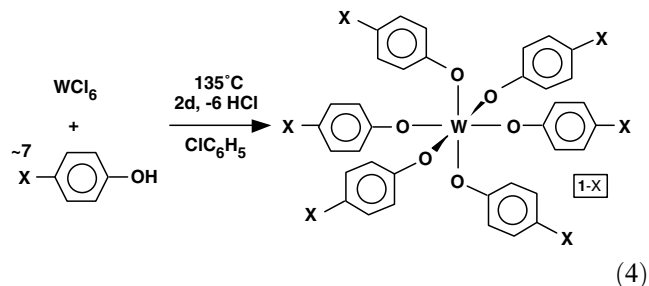
at 213 °C in a bomb reactor yielded the polybenzyl ether, (*p*-PhCH₂OC₆H₄O)₆W (**1-OCH₂Ph**, 91%). Deprotection via hydrogenation (H₂ (1 atm), Pd/C) in ethanol/toluene ultimately yielded dark red (*p*-HOC₆H₄O)₆W·2THF·C₆H₆ ((**1-OH**)·2THF·C₆H₆) upon crystallization from THF/benzene. A structural investigation of (**1-OH**)·2THF·C₆H₆ revealed a dense 3-D hydrogen-bonding network linking phenolic and THF sites. The addition of Lewis bases such as 4,4'-bipyridine and 1,2-di-4-pyridylethane to **1-OH** led to the hexabasic mononuclear complex (4,4'-bipy·HOC₆H₄O)₆W (**2**), the doubly interpenetrating 3-D network [{W(OC₆H₄OH)₆}{4,4'-(NC₅H₄)₂(CH₂CH₂)₂}₂]_∞ (**3**), and the triply interpenetrating 3-D network [{W(OC₆H₄OH)₆}{4,4'-(NC₅H₄)₂(CH₂CH₂)₃·THF}]_∞ (**4**·THF), according to X-ray crystallographic studies [33].

While the network solids were intriguing, the stabilization of pendant hydroxy functionalities on a high valent early transition metal center was a striking observation. Earlier studies of group 4 and 5 derivatives suggested that self-condensation was prevalent, yet no oligomerization chemistry was evident for (*p*-HOC₆H₄O)₆W (**1-OH**). Now that the hydroxy functional group could be engineered into the W(VI) center, could reactivity other than hydrogen bond formation be exploited?

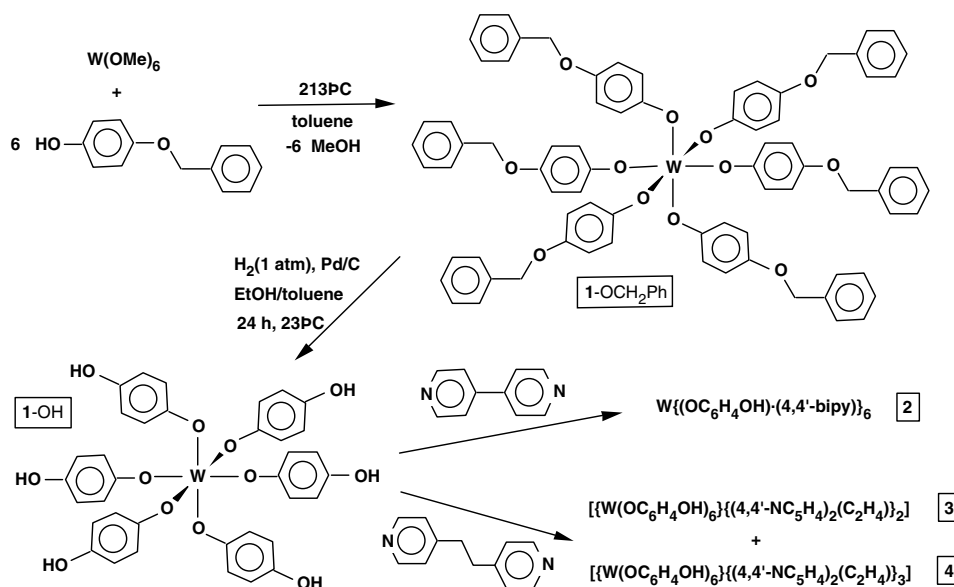
2.1.2. (*p*-XC₆H₄O)₆W (**1-X**), (*p*-XC₆H₄O)₅W(OC₆H₄OCH₂Ph) (**5-X**) and (*p*-XC₆H₄O)₅W(OC₆H₄OH) (**6-X**), X = H, CH₃, OCH₃, Cl, Br)

para-Substituted tungsten hexaphenoxide complexes were synthesized via modification of methods developed by Beshouri and Rothwell [34], which in turn were mod-

est variants of Funk and Baumann [35], and Mortimer and Strong [36]. Treatment of tungsten hexachloride with ~7 equiv. of *p*-XC₆H₄OH in refluxing chlorobenzene for 2 d formed (*p*-XC₆H₄O)₆W (**1-X**, X = H, 82%; CH₃, 60%; OCH₃, 40%; Cl, 87%; Br, 68%) in varying yields.



Since an entire [(*p*-XC₆H₄O)₅W] unit was considered as a tunable group for the ensuing electrochemical study, a protocol for the replacement of one phenoxide from **1-X** was needed. As Scheme 2 reveals, (*p*-XC₆H₄O)₆W reacted with HOC₆H₄OCH₂Ph in refluxing chlorobenzene with catalytic tosylic acid to yield a mixture of substituted products, (*p*-XC₆H₄O)_{6-x}W(OC₆H₄O-CH₂Ph)_x (*x* = 1, **5-X**), as determined by TLC. The mixture of substituted products was hydrogenated (10% Pd/C, 1 atm H₂) in an EtOH/toluene mixture to a mixture of hydroxylated products, (*p*-XC₆H₄O)_{6-x}W(OC₆H₄OH)_x (*x* = 1, **6-X**), also determined by TLC. The mono-hydroxylated species **6-X** were separated from the mixture by column chromatography and recrystallized from ethanol (X = H, 19%; Me, 29%; OCH₃, 19%; Cl, 12%; Br, 11%).



Scheme 1.

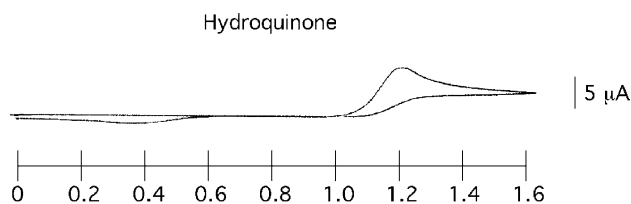
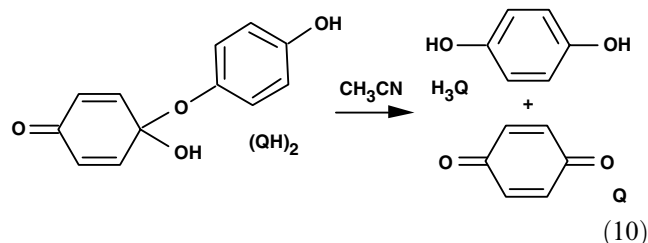
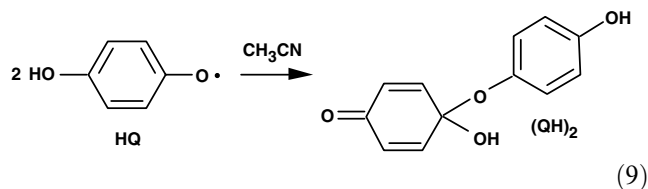


Fig. 2. Cyclic voltammogram of hydroquinone in acetonitrile: 0.5 mM QH₂, 0.1 M TBAH (tetra-*n*-butylammonium hexafluorophosphate), Ag wire reference, 100 mV/s.

Fig. 2 shows the oxidation of hydroquinone at platinum electrodes in acetonitrile. The peak potential of the irreversible oxidation wave (wave I, +1.40 V versus NHE) and irreversible reduction wave (wave II, +0.55 V versus NHE) were similar to the values reported by Chambers and Eggins [37] (wave I, +1.36 V; wave II, +0.37 V versus NHE, 2 V/s), who found that the peak potential and width for wave II was highly dependent on scan rate and pH. Further investigation into the behavior of wave I led to a proposed mechanism whereby reversible one electron oxidation of hydroquinone (QH₂) forms the radical cation QH₂^{•+} (Eq. (6)) followed by rapid, irreversible deprotonation to the protonated semiquinone QH (Eq. (7)). A hemiketal intermediate (QH)₂ then forms via HQ dimerization (Eq. (9)), followed by disproportionation to yield Q and H₂Q (Eq. (10))



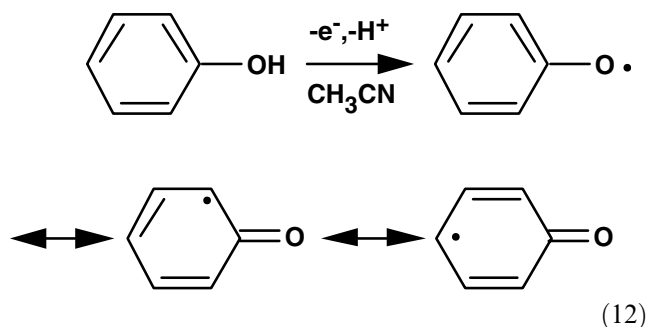
Wave II is the irreversible two electron reduction of the Q/H⁺ mixture back to hydroquinone (Eq. (11)) [9]



2.2.2. Phenols

The oxidation of phenols can lead to a variety of products depending on the oxidant, catalyst, or substitution pattern of the phenol [39]. Treatment of 2,6-xyleneol with a copper pre-catalyst in the presence of dioxygen yielded either diphenoquinone or polyphenylene ether depending on the pyridine to cuprous chloride ratio

[40]. Lau and coworkers have found that in both water and acetonitrile oxidation of *p*-XC₆H₄OH (X = MeO, ^tBu, Me, Cl, CN, H) by *trans*-[Ru^{VI}(L)(O)₂]²⁺ (L = 1,12-dimethyl-3,4:9,10-dibenzo-1,12-diaza-5,8-dioxacyclopentadecane) proceeds via a hydrogen atom abstraction mechanism. The unstable phenoxy radical was further oxidized to *p*-benzoquinone and 4,4'-biphenoquinone via rapid competing steps [41]. Electrochemical studies on the mechanism of phenol oxidation suggest that the first step is an irreversible one electron oxidation of phenol followed by proton loss forming the resonance stabilized phenoxy radical shown in Eq. (12) [42]



2.2.3. (*p*-XC₆H₄O)₆W (1-X, X = H, CH₃, OCH₃, Cl, Br, OH), (*p*-XC₆H₄O)₅W(OC₆H₄OH), and *p*-XC₆H₄OH

The impetus for attempting this project stemmed from three observations. First, cyclic voltammetry on (*p*-HOC₆H₄O)₆W (1-OH) revealed multiple irreversible oxidation waves at ~1.29 V (versus NHE) and 1.63 V (Table 1). According to Fig. 1, if these events were indicative of a process such as that in Eq. (8), which is expected to be irreversible in analogy to H₂Q/Q electrochemistry, then C–H bonds of considerable strength could conceivably be attacked. In order to simplify the system, and to modulate the oxidation potentials of interest through *para*-substitution, (*p*-XC₆H₄O)₅W(OC₆H₄OH) (6-X, X = H, CH₃, OCH₃, Cl, Br) were synthesized. Second, a 0.0–2.3 V (versus Ag wire) cyclic voltammogram of (*p*-BrC₆H₄O)₅W(OC₆H₄OH) (6-Br), which was chosen because it possesses a second oxidation wave at ~+1.95 V (versus NHE), showed a pronounced increase in current when excess Ph₃CH (3–10 equiv.; BDE ~ 81 kcal/mol) [43] was added to the solution. In concert with this experiment, the addition of dihydroanthracene (BDE ~ 79 kcal/mol) [31] to a solution of (*p*-ClC₆H₄O)₅W(OC₆H₄OH) (6-Cl) caused a similar increase in current at ~+1.9 V (versus NHE) during another 0.0–2.3 V scan.

In view of the possibility of electrocatalytic C–H bond activation, some other cases seemed puzzling. Under similar conditions, no evidence of toluene (BDE ~ 89.8(6) kcal/mol) [43] or acetonitrile

Table 1

 E_{red}^0 and E_{ox}^0 values (V vs. NHE, CH₃CN)^a for p -XC₆H₄OH, (p -XC₆H₄O)₆W (**1-X**) and (p -XC₆H₄O)₅W(OC₆H₄OH) (**6-X**); X = H, Me, OMe, Cl, Br

Compound vs. NHE (V)	$E_{\text{red}}(1)$	$E_{\text{red}}(2)$	$E_{\text{ox}}(1)$	$E_{\text{ox}}(2)$ ^b
(p -BrC ₆ H ₄ O) ₆ W (1-Br)	-0.17	-1.22	1.88 ^c	2.2
(p -BrC ₆ H ₄ O) ₅ W(OC ₆ H ₄ OH) (6-Br)	-0.16	-1.19	1.32 ^b	1.95
p -BrC ₆ H ₄ OH	-1.61		2.03	
(p -ClC ₆ H ₄ O) ₆ W (1-Cl)	-0.17	-1.28	1.84	2.2
(p -ClC ₆ H ₄ O) ₅ W(OC ₆ H ₄ OH) (6-Cl)	-0.28	-1.35	1.41	1.91
p -ClC ₆ H ₄ OH	-1.25		1.95	
(C ₆ H ₅ O) ₆ W (1-H)	-0.4	-1.6	1.83	
(C ₆ H ₅ O) ₅ W(OC ₆ H ₄ OH) (6-H)	-0.26	^d	1.45	^d
C ₆ H ₅ OH	-1.89		2.24	
(p -MeC ₆ H ₄ O) ₆ W (1-Me)	-0.59	-1.70	1.47	^e
(p -MeC ₆ H ₄ O) ₅ W(OC ₆ H ₄ OH) (6-Me)	-0.54	-1.62	1.26	^f
p -MeC ₆ H ₄ OH	-1.85		1.73	
(p -MeOC ₆ H ₄ O) ₆ W (1-OMe)	-0.54	-1.5	1.33	1.71 ^g
(p -MeOC ₆ H ₄ O) ₅ W(OC ₆ H ₄ OH) (6-OMe)	-0.56	-1.63	1.17	1.72 ^g
p -MeOC ₆ H ₄ OH	-1.57		1.52	
(p -HOC ₆ H ₄ O) ₆ W (1-OH)	-0.58	-1.75	1.29 ^c	1.63
p -HOC ₆ H ₄ OH	0.55		1.40	

^a From cyclic voltammetry referenced to Ag wire with 0.1 M added tetra-*n*-butylammonium hexafluorophosphate (TBAH); the tabulated values are vs. NHE because the thermodynamic quantities in Fig. 1 use NHE as a reference. Typical samples were ~0.5 mM, and all scan rates were 100 mV/s.

^b Appear as shoulders atop a generally featureless, increasing current.

^c Multiple waves.

^d Scan was only from -1.6 to +1.8 V.

^e Possible shoulder at +1.9 V.

^f Scan to 2.0 V, current still increasing.

^g Other minor waves visible.

(BDE ~ 94.8(21) kcal/mol) [43] activation by any **6-X** species was noted, despite oxidation potentials that suggested such events were feasible according to the calculations of Fig. 1. It was also plausible that toluene might be activated by hydride transfer, but while a cycle similar to that in Fig. 1 can be constructed [44], not enough thermodynamic parameters are known for $\text{RH} \rightarrow \text{R}^+ + \text{H}^-$ to determine its feasibility. Regardless, cyclic voltammograms of **6-X** in the presence of toluene were unchanged. Finally, Fig. 4 illustrates another CV of (p -BrC₆H₄O)₅W(OC₆H₄OH) (**6-Br**) taken from -2.2 to +2.3 V; when cycled in the presence of Ph₃CH, *this voltammogram was unchanged*. Whatever was generated in Fig. 3 does not persist when the scan is taken to -2.2 V for the longer period associated with it (Fig. 4).

Table 1 lists the electrochemical reduction and oxidation waves attributed to (p -XC₆H₄O)₆W (**1-X**, X = H, CH₃, OCH₃, Cl, Br, OH), (p -XC₆H₄O)₅W(OC₆H₄OH) (**6-X**), and p -XC₆H₄OH. In general, the phenols exhibit an irreversible oxidation wave (two in some cases) that increases in potential according to substituent from π -donors to σ -donors to σ -withdrawing groups: p -X = OH (easiest) < OMe < Me < Cl < Br < H. The oxidation wave appears as a featureless increase in current that is initiated at high potentials. The differences based on substituent are substantial, span 0.84 V, and the parent phenol is oxi-

dized at an anomalously high potential of +2.24 V. Presumably Cl < Br because the former has some π -influence that contradicts its σ -effect. Ignoring hydroquinone and its special characteristics (vide supra), the phenols also exhibit a quasi-reversible reduction wave. Here the inductive contributions appear to play a greater role than any π -effects because the ease of reduction follows p -X = Cl (easiest) > OMe > Br > Me > H, and the range of potentials is 0.64 V. π -Type electrons on substituents are energetically closer to arene π -bonding orbitals than arene π^* -orbitals. As a consequence, π -effects play a greater role facilitating oxidation of the phenols. The reduction trend sim-

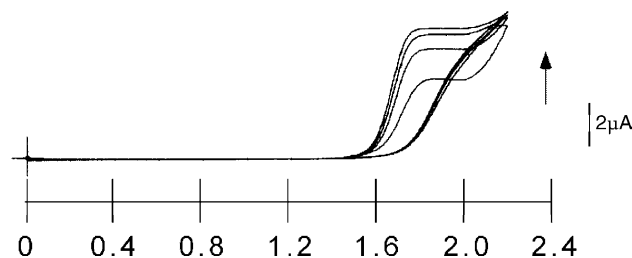


Fig. 3. Cyclic voltammogram of (p -BrC₆H₄O)₅W(OC₆H₄OH) (**6-Br**) in CH₃CN showing the increase in current in successive scans after addition of Ph₃CH (~5 mM): ~0.5 mM **6-Br**, 0.1 M TBAH (ⁿBu₄PF₆), Ag wire reference, 100 mV/s.

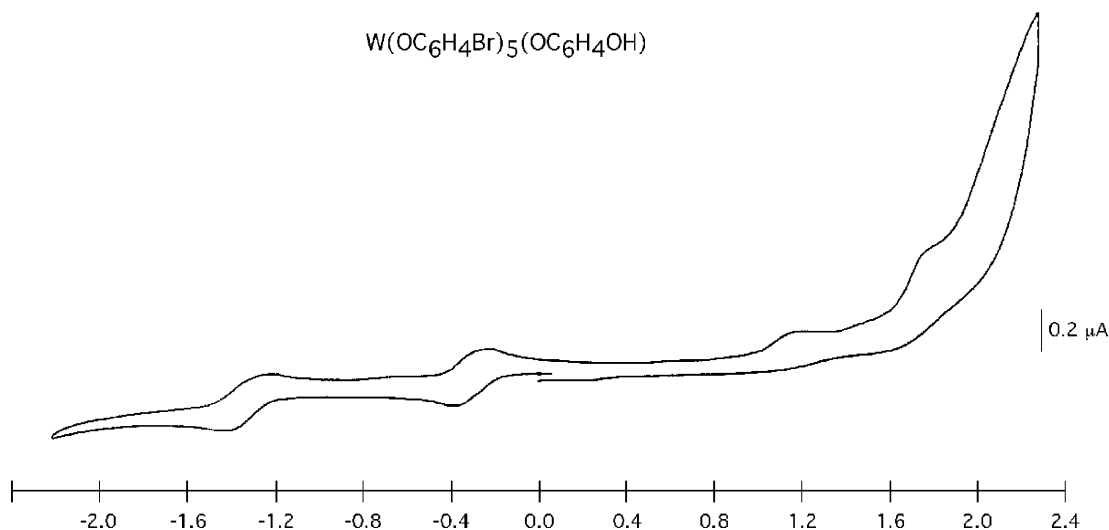


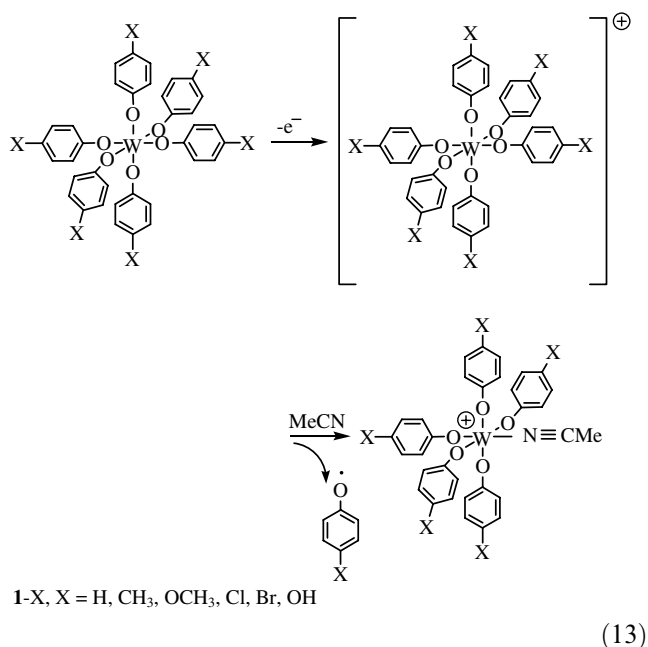
Fig. 4. Cyclic voltammogram of $(p\text{-BrC}_6\text{H}_4\text{O})_5\text{W(OC}_6\text{H}_4\text{OH)}$ (**6-Br**) in acetonitrile from -2.2 to $+2.3$ V: ~ 0.5 mM **6-Br**, 0.1 M TBAH (tetra-*n*-butylammonium hexafluorophosphate), Ag wire reference, 100 mV/s.

ply reflects inductive effects, which will tend to lower both the donor π -orbitals and the receptor π^* -orbitals of the phenols as the substituents become more electron-withdrawing.

As previously observed for related compounds by Beshouri and Rothwell [34], $(p\text{-XC}_6\text{H}_4\text{O})_6\text{W}$ (**1-X**, X = H, CH₃, OCH₃, Cl, Br, OH) exhibit two reversible reduction waves corresponding to the formation of anions $[\mathbf{1-X}]^-$ and dianions $[\mathbf{1-X}]^{2-}$. In contrast to the phenols, these reductions reflect a substantial influence by π -components, which render the reductions more difficult. The trend of ease of the first reduction for **1-X** is $p\text{-X} = \text{Br} \sim \text{Cl}$ (easiest) $> \text{H} > \text{OMe} > \text{OH} > \text{Me}$, and the range of potentials is 0.42 V. Inductively, the oxygenated substituents should be on par with Cl, but their π -donor capability renders them more difficult to reduce. The trend of the second reduction has roughly the same range (0.53 V) and the trend is also similar: $p\text{-X} = \text{Br}$ (easiest) $> \text{Cl} > \text{OMe} > \text{H} > \text{Me} > \text{OH}$. π -Donors increase the π -donating ability of the phenoxides, which results in an increase in energy of the t_{2g} receptor orbitals on the pseudo-octahedral complexes. This counteracts the tendency of σ -withdrawing substituents to lower the t_{2g} set. The reductions can certainly be rationalized as metal in character, and quite different from the phenols.

The oxidations of $(p\text{-XC}_6\text{H}_4\text{O})_6\text{W}$ (**1-X**, X = H, CH₃, OCH₃, Cl, Br, OH) are complicated. A relatively clean irreversible wave ($E_{\text{ox}}(1)$) occurs for $p\text{-X} = \text{OH} < \text{OMe} < \text{Me} < \text{H} \sim \text{Cl} < \text{Br}$, which is basically the same trend – corresponding to the same effects – seen for the aforementioned phenol oxidations. The values are slightly less positive by 0.1–0.4 V, consistent with removal of an electron from ligand-based orbitals that are more “phenolate” in character. During and after this

oxidation, there is a large increase in current, often with no readily discernable peak. The second oxidation ($E_{\text{ox}}(2)$), if it is clear, appears as a wave atop this increase. In the cyclic voltammogram of **1-Br** shown in Fig. 5, both oxidation waves are atop the current increase. The $E_{\text{ox}}(2)$ values, when clearly observed, reflect the previous trend. The similarities in $E_{\text{ox}}(2)$ and the oxidation waves of the parent phenols strongly suggest that the current increase observed is due to degradation of **1-X** and the release of phenol via phenoxy radical



The reductions of $(p\text{-XC}_6\text{H}_4\text{O})_5\text{W(OC}_6\text{H}_4\text{OH)}$ (**6-X**, X = H, CH₃, OCH₃, Cl, Br) are essentially the same as

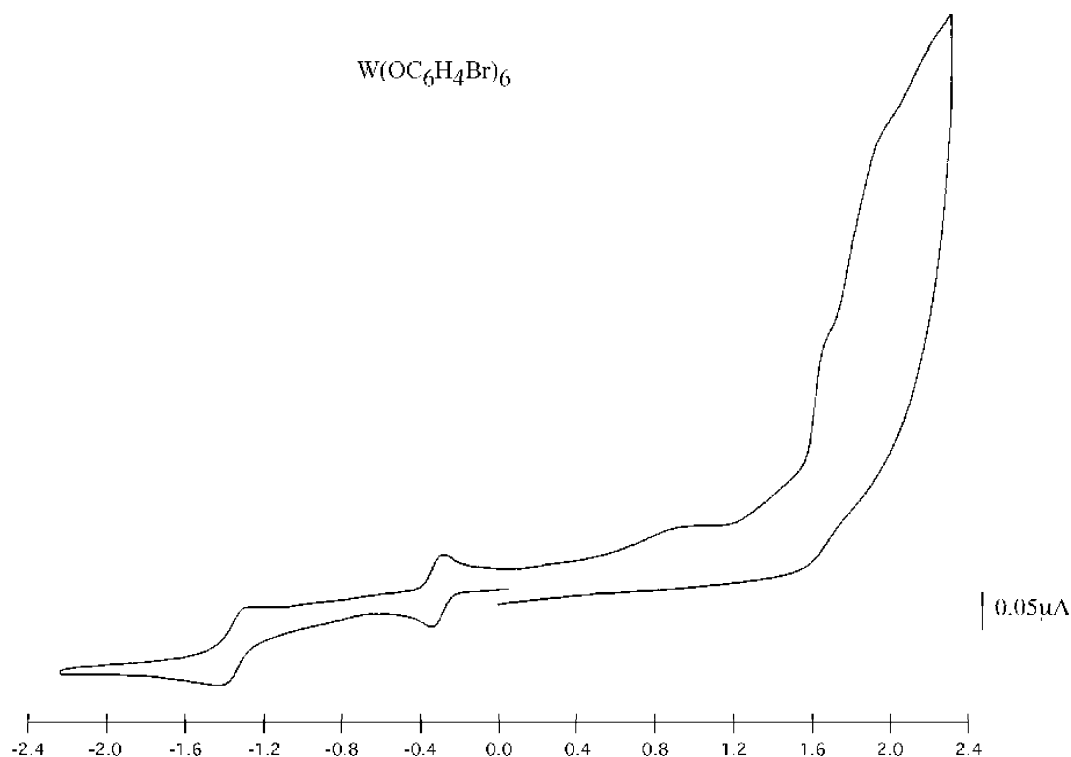


Fig. 5. Cyclic voltammogram of $(p\text{-BrC}_6\text{H}_4\text{O})_6\text{W}$ (**1-Br**) in acetonitrile from -2.2 to $+2.3$ V: ~ 0.5 mM **1-Br**, 0.1 M TBAH (tetra-*n*-butylammonium hexafluorophosphate), Ag wire reference, 100 mV/s.

those of **1-X** within 0.1 V. The oxidations appear to reveal the problem in implementing electrocatalytic C–H bond activation. Each complex has an irreversible oxidation around $+1.2$ to 1.5 V that appears essentially at the onset of a large current increase. This is likely to be the oxidation of the *p*- $\text{HOC}_6\text{H}_4\text{O}$ -ligand, since it is very close to the oxidations of **1-OH** and that of hydroquinone. The second oxidation, when observed atop the current increase, is near that of $E_{\text{ox}}(2)$ of **1-X** and the phenols. It is plausible that initial oxidation occurs at the *p*- $\text{HOC}_6\text{H}_4\text{O}$ -ligand, perhaps via a process like that revealed in Eq. (8). If the W(V) quinone product (or W(VI) semiquinone) degrades before H atom abstraction can occur to regenerate **6-X**, degradation would lead to phenol loss. While the initial oxidation wave can be attributed to the $\text{HOC}_6\text{H}_4\text{O}$ -ligand, a wave that would correspond to the reduction of free quinone is *not* evident, thus it is likely that protons generated upon oxidation are playing a role in the degradation.

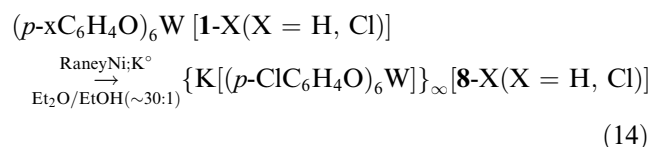
Detection of phenol atop the general increase in current, which probably reflects the production of a number of oxidizable species, is a likely signature of catastrophic degradation.

2.3. Attempted generation of $(\text{XC}_6\text{H}_4\text{O})_5\text{W}(\text{OC}_6\text{H}_4\text{O})$ (**7-X**)

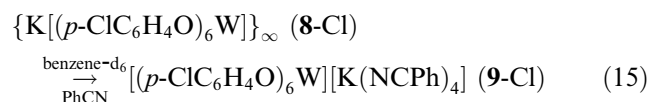
Although electrocatalytic C–H bond activation via Fig. 1 was not realized, it was still possible that the

W(V) quinone/W(VI) semiquinone complex, $(p\text{-XC}_6\text{H}_4\text{O})_5\text{W}(\text{OC}_6\text{H}_4\text{O})$ (**7-X**, X = H, CH_3 , OCH_3 , Cl, Br, OH) was generated yet unstable under the electrochemical conditions. Early work suggested that the in situ preparation of **7-X** could be undertaken by utilizing a W(V) precursor. Funk et al. indicated that the reduction of $(p\text{-XC}_6\text{H}_4\text{O})_6\text{W}$ (**1-X**, X = H, CH_3 , Cl) by Raney nickel in the presence of potassium metal produced the five coordinate tungsten(V) aryloxides, “ $(p\text{-XC}_6\text{H}_4\text{O})_5\text{W}$ ” [45]. Despite product characterization that included molecular weight determination, EA, EPR and polarography, a five coordinate complex of this type would seem to be sterically capable of dimerizing to form $[(p\text{-XC}_6\text{H}_4\text{O})_4\text{W}]_2(\mu\text{-OC}_6\text{H}_4\text{X})_2$. Later work by Wilkinson and coworkers [46] showed that reduction of $\text{W}(\text{OPh})_6$ by metallic lithium, sodium, or potassium in THF produced the octahedrally coordinated hexaphenoxotungstate(V) ion $[\text{W}(\text{OPh})_6]^-$ as $[\text{Li}(\text{thf})_2][\text{W}(\text{OPh})_6]$, $[\text{Na}][\text{W}(\text{OPh})_6] \cdot \text{NaOPh}$, and $[\text{K}][\text{W}(\text{OPh})_6]$, respectively. The monomers $[\text{Et}_4\text{N}][\text{W}(\text{OPh})_6]$, formed by treating $\text{Na}[\text{W}(\text{OPh})_6] \cdot \text{NaOPh}$ with excess $[\text{Et}_4\text{N}]\text{Br}$, and $[\text{Li}(\text{thf})_2][\text{W}(\text{OPh})_6]$ were structurally characterized. EPR spectra were collected in frozen tetrahydrofuran at 100K for all of the $[\text{W}(\text{OPh})_6]^-$ compounds as well as “ $(\text{PhO})_5\text{W}$ ”, and the values appeared similar. Wilkinson and coworkers [46] proposed that “ $(\text{PhO})_5\text{W}$ ” in THF was most likely the axially distorted W^{V} monomer $\text{W}(\text{OPh})_5(\text{thf})$, although no further characterization was reported.

Following the Funk protocol [45], reduction of (*p*-ClC₆H₄O)₆W (**1-Cl**) with Raney Ni (Et₂O:EtOH; 40:1) generated a red solution that turned yellow-orange upon addition of K⁰. The addition of quinone caused an immediate color change to purple-red, and a black solid precipitated. ¹H NMR spectroscopy revealed only the formation of **1-Cl**. Since the solvent system appeared incompatible, the procedure was redone in Et₂O and THF-d₈ with similar results. As Eq. (14) shows, in Et₂O the reduction procedure yields {K[(*p*-XC₆H₄O)₆W]}_∞ (**8-X**, X = H, 44%; Cl 61%) which can be isolated as orange crystals in 61% yield



Attempts to remove one of the phenoxide ligands from {K[(*p*-ClC₆H₄O)₆W]}_∞ (**8-Cl**) by electrophilic attack with [Me₃O][BF₄] or Me₃SiCl only resulted in oxidation to (*p*-ClC₆H₄O)₆W (**1-Cl**). The phenoxide ligand resisted substitution by PhCN, but ¹H NMR spectroscopy indicated that benzonitrile breaks up the infinite chain into a monomeric species, [(*p*-ClC₆H₄O)₆W][K(NCPh)₄] (**9-Cl**, Eq. (15))



2.4. X-ray crystal structure of {K[(*p*-ClC₆H₄O)₆W]}_∞ (**8-Cl**)

Crystallographic data for {K[(*p*-ClC₆H₄O)₆W]}_∞ (**8-Cl**) are presented in Table 2 and pertinent interatomic distances and angles are listed in Table 3. As Fig. 6 reveals, **8-Cl** forms a zig-zag chain of [(*p*-ClC₆H₄O)₆W][−] anions and potassium cations. The potassium cation is coordinated by a distorted square plane of oxygen atoms (∠O–K–O_{cis} = 55.8(1)°, 124.2(1)°; ∠O–K–O_{trans} = 180°) in addition to axial coordination by two asymmetrically bound aryl rings of two different [(*p*-ClC₆H₄O)₆W][−] units (Fig. 7). A small distortion from octahedral coordination is observed in the WO₆ core (∠O1–W1–O2 = 87.8(1)°; ∠O1–W1–O3 = 91.4(1)°; ∠O2–W1–O3 = 92.4(1)°) (Fig. 8). The average W–O bond distance (1.955(1) Å) is longer than the average distance of normal tungsten(VI) aryloxy bonds (1.889(14) Å) [33,47] reflecting partial population of the π* orbitals of d¹ pseudo-octahedral W(V). A shorter terminal W–O bond distance (1.946(1) Å) is found in comparison to the bridged W–O distances (*d*(W1–O1) = 1.960(2) Å; *d*(W1–O2) = 1.959(1) Å).

Table 2
Crystallographic data for triclinic {K[(*p*-ClC₆H₄O)₆W]}_∞ (**8-Cl**)

Formula	C ₃₆ H ₂₄ O ₆ Cl ₆ KW
Formula weight	494.10
Space group	<i>P</i> $\bar{1}$
λ (Å)	0.71073
<i>a</i> (Å)	7.7888 (4)
<i>b</i> (Å)	10.3052 (6)
<i>c</i> (Å)	11.8888 (7)
α (°)	100.7200 (10)
β (°)	105.4990 (10)
γ (°)	96.7620 (10)
<i>V</i> (Å ³)	889.26 (9)
<i>T</i> (K)	173(2)
<i>Z</i>	1
ρ_{calc} (g/cm ³)	1.845
μ (mm ^{−1})	3.862
<i>R</i> [<i>I</i> > 2 σ (<i>I</i>)] ^a	0.0218
<i>w</i> ² [<i>I</i> > 2 σ (<i>I</i>)] ^b	0.0558
Goodness-of-fit ^c	1.028
Largest differential peak (e [−] Å ^{−3})	1.740
Largest differential hole (e [−] Å ^{−3})	−1.188

^a $R_1 = \sum[|F_o| - |F_c|] / \sum|F_o|$.

^b $wR_2 = [\sum w(|F_o| - |F_c|)^2 / \sum w F_o^2]^{1/2}$.

^c GOF = $[\sum w(|F_o| - |F_c|)^2 / (n - p)]^{1/2}$, *n* = number of independent reflections (5665 of 12 570, *R*_{int} = 0.0237), *p* = number of parameters (277).

3. Discussion

3.1. Radical CH bond activation

3.1.1. Electrocatalyst lifetime

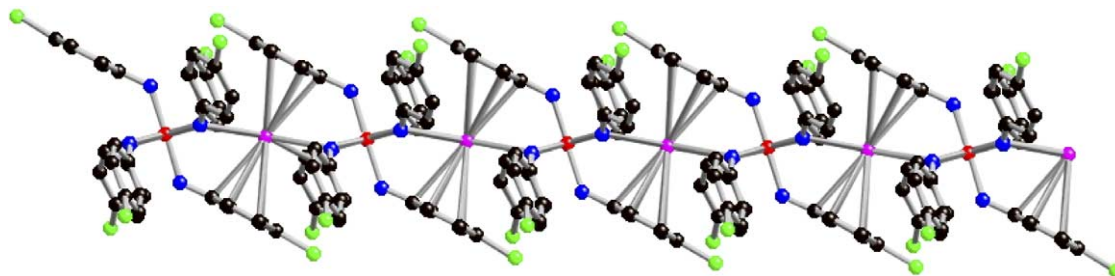
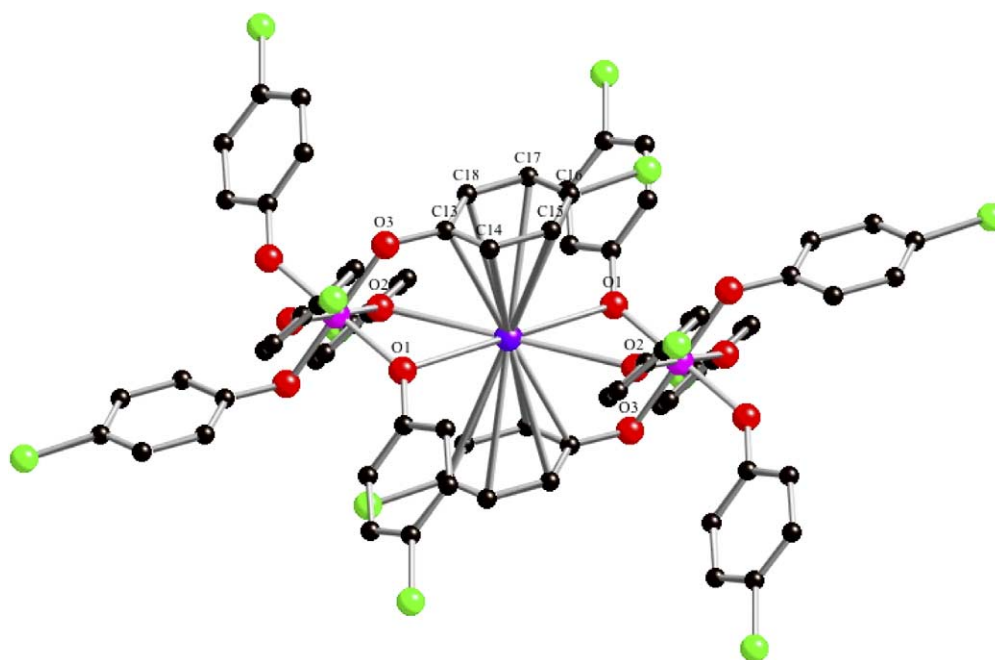
The premise of this project, electrocatalytic CH bond activation, was not realized. In an electrocatalytic process [4], either reduction or oxidation (this case) serves to regenerate a complex that undergoes a redox process, hence the electrode takes the place of a chemical redox partner that would be consumed (e.g., dioxygen) in the reaction. Rapid degradation of the electrochemically generated W(V) quinone or alternately described W(VI) semiquinone radical intermediate prior to H atom abstraction was considered as one possible cause of failure. In Fig. 3, the short potential range (0.0–2.3V) allowed degradation products (probably phenols) to be regenerated with a H atom source present, whereas the longer potential range in Fig. 4 (−2.2 to 2.3 V) and longer scan time yielded no behavior that could be misconstrued as “electrocatalytic”.

In retrospect, the lifetime of the intermediate that must do the H atom abstraction must be substantial, and this factor was underappreciated in this study. For example, according to an Evans–Polanyi plot [48], the activation of dihydroanthracene by transient (*p*-XC₆H₄O)₅W(O-C₆H₄O) (**7-X**, X = H, CH₃, OCH₃, Cl, Br, OH) that was formed from *E*_{ox}⁰ ~ +1.4 V (Fig. 1) would occur at roughly 10 M^{−1} s^{−1}, hence the lifetime of **7-X** would need to be around a tenth

Table 3

Selected interatomic distances (Å) and angles (°) pertaining to $\{K[(p\text{-ClC}_6\text{H}_4\text{O})_6\text{W}]\}_\infty$ (8-Cl)

Interatomic distances					
W–O1	1.874 (3)	K1–C13	3.139 (2)	K1–C14	3.270 (2)
W–O2	1.926 (3)	K1–C15	3.538 (2)	K1–C16	3.652 (2)
W–O3	1.913 (2)	K1–C17	3.516 (2)	K1–C18	3.257 (2)
(K–O) _{ave}	2.904 (2)				
Interatomic angles					
(O–W1–O) _{trans}	180	O1–W1–O2	87.8 (1)	O1–W1–O3	91.4 (1)
O2–W1–O3	92.4 (1)	W1–O1–C1	135.0 (1)	W1–O2–C7	139.1 (1)
W1–O3–C13	132.3 (1)	O1–K–O2	55.8 (1)	O1–K–O2'	124.2 (1)

Fig. 6. Molecular view of the extended structure of $\{K[(p\text{-ClC}_6\text{H}_4\text{O})_6\text{W}]\}_\infty$ (8-Cl). W, purple; K, blue; O, red; Cl, green; C, black.Fig. 7. Coordination environment of K cation in $\{K[(p\text{-ClC}_6\text{H}_4\text{O})_6\text{W}]\}_\infty$ (8-Cl).

of a second; at 2.1 V, activation would occur at $\sim 10^6 \text{ M}^{-1} \text{ s}^{-1}$ and its lifetime would need to be in the microsecond range. All oxidation waves found for $(p\text{-XC}_6\text{H}_4\text{O})_5\text{W}(\text{OC}_6\text{H}_4\text{OH})$ (6-X, X = H, CH₃, OCH₃, Cl, Br; X = OH, 1-OH) on the 100 mV/s timescale were irreversible, and no reproducible reduction waves were ever seen in this region, even at higher scan speeds (100 V/s). Given the failure to achieve activation, no further elucidation of the electrochemistry or product analyses were attempted.

3.1.2. Solvent stability and ionization energy

An attempt at CH bond activation using an electrocatalytic cycle requires the use of a solvent that will support an electrolyte and not suffer activation. One might question the utility of such a process given the rather low BDEs of polar solvents such as acetonitrile (BDE $\sim 94.8(21)$ kcal/mol, ~ 19 M) [43]. From the calculations in Fig. 1 acetonitrile should have been an excellent substrate for the putative quinone based chemistry projected for 6-X.

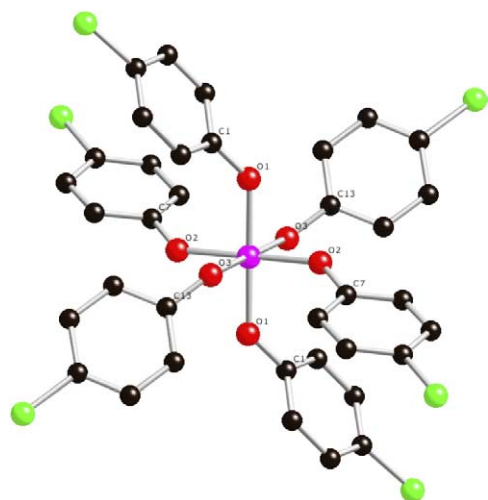


Fig. 8. Molecular view of the $[(p\text{-ClC}_6\text{H}_4\text{O})_6\text{W}]^-$ ion in $\{\text{K}[(p\text{-ClC}_6\text{H}_4\text{O})_6\text{W}]\}_\infty$ (8-Cl).

Que has examined the remarkable oxidation of hydrocarbons by non-heme Fe(IV) oxo compounds in acetonitrile, thereby providing evidence to the contrary [27]. Que et al. generate $[\{(\text{pyCH}_2)_2\text{NCH}_2\text{CH}_2\text{N}(\text{CH}_2\text{py})_2\}\text{FeO}]^{2+}$ ($[(\text{Bn}\text{-tpen})\text{FeO}]^{2+}$) in acetonitrile and measure second-order rate constants for the activation of several hydrocarbons, including cyclohexane, apparently without competition from solvent activation. They correlate the $\log k(\text{act})$ versus the BDE(substrate) in the usual fashion, but had acetonitrile been included as a “substrate”, it would stand out as a dramatically outlying point. If one estimates the reaction of $[(\text{Bn}\text{-tpen})\text{FeO}]^{2+}$ with acetonitrile as the compound’s decomposition rate, one can rationalize the inexplicable stability of acetonitrile to H atom abstraction.

Fig. 9 plots the $\ln k_2$ (k_2 in $\text{M}^{-1} \text{s}^{-1}$) versus IE (eV) for the substrates used and acetonitrile, assuming its activation rate is that of the Fe(IV) oxo’s degradation in the absence of added substrate [27]. A clean correlation is observed, with $R^2 = 0.955$; CH_2Cl_2 , which is not used in Que’s study, but has seen use in radical-based systems, is given a predicted activation $\ln k_2$ based on its IE. This plot is a reasonable alternative to the more conventional $\log k_2$ versus BDE employed by Que, and has the obvious advantage of being able to include acetonitrile, yet what is its interpretation?

In Fig. 10, two reaction paths for H atom abstraction are given: one implicates a synchronous transfer of proton and electron, and one reveals a transition state (e.g., the half-way point) that consists of greater electron transfer character than proton transfer. In such an instance, electron withdrawing groups on the substrate, such as the CN on acetonitrile or the chlorides on CH_2Cl_2 can attenuate the susceptibility to H atom abstraction, despite BDEs that would lead one to predict ready activation. Note that a non-synchronous

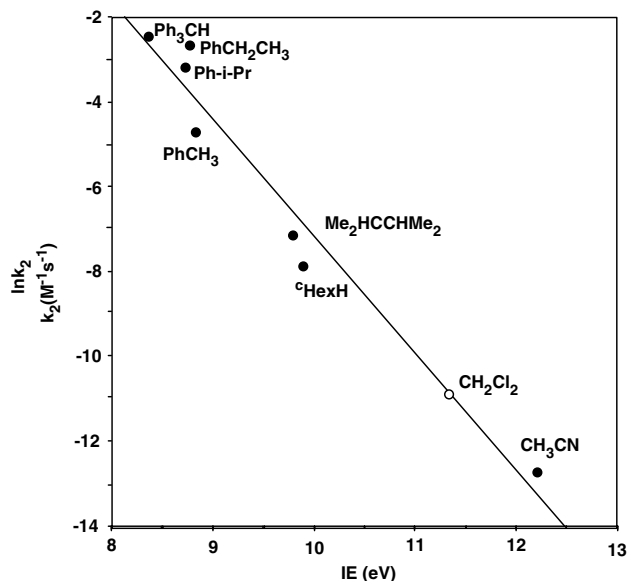


Fig. 9. Correlation of Que et al. hydrocarbon activation rates (k_2 in $\text{M}^{-1} \text{s}^{-1}$) by $[(\text{Bn}\text{-tpen})\text{FeO}]^{2+}$ vs. IE (eV), assuming its degradation rate is that of CH_3CN activation. An estimate of methylene chloride activation based on its IE is given as an open circle.

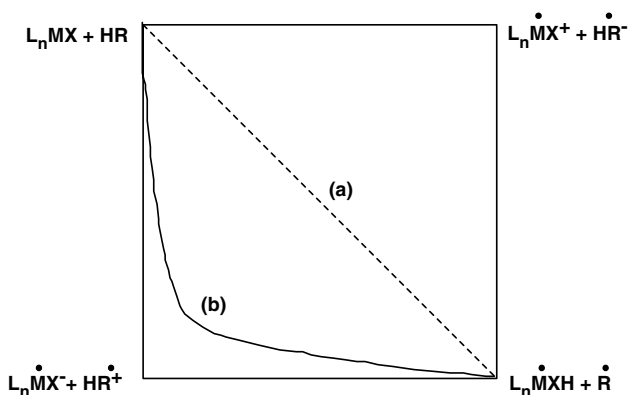


Fig. 10. Reaction coordinate for H atom transfer to L_nMX comparing: (a) direct path where the proton and electron travel simultaneously and (b) a path that possesses more electron transfer character at the transition state.

transfer could lower the frequencies of transition state vibrations that contribute heavily to the kinetic isotope effect (KIE) for H atom transfer (i.e., frequencies of a transition state with RH^+ character should be lowered considerably from that of R^\cdot). It has been shown that such low frequency vibrations are a significant contributor to some anomalously high KIEs [49].

3.2. Phenoxide complexes

The stability of tungsten *para*-hydroxy-phenoxide complexes to degradation via oligomerization and

condensation permitted the synthesis of $(p\text{-XC}_6\text{H}_4\text{O})_5\text{W}(\text{O-C}_6\text{H}_4\text{OH})$ (**6-X**, X = H, CH₃, OCH₃, Cl, Br; X = OH, 1-OH) for this study. Their stability to excessive proton-induced ligand exchange, and chromatography conditions verifies their robust character. The complexes and their hexaphenoxide precursors exhibit clean, reversible reductions to anionic and dianionic species, but oxidations were irreversible and induced degradation. It was disappointing that variation of the $(p\text{-XC}_6\text{H}_4\text{O})_5\text{W}$ fragment failed to substantially change the oxidation potential of the $-\text{OC}_6\text{H}_4\text{OH}$ group, which was the first oxidation wave in each **6-X**, despite the wide variation in the oxidation potentials of the parent phenols. It was hoped that the variation in phenol oxidation potential would be transmitted to some extent to the W center and amplified given the five $p\text{-XC}_6\text{H}_4\text{O}$ ligands, but this was not observed.

If one views the $\text{WOC}_6\text{H}_4\text{OH}$ unit as a “phenoxide anion”, precedent suggests that the premise of this study was thermodynamically doomed. Cheng et al. calculated several p -hydroquinone anion bond strengths to be $\sim 66\text{--}74$ kcal/mol, which are values incommensurate with the proposed CH bond activation. This work is certainly consistent with the relatively steady, irreversible $E_{\text{ox}}^0(1)$ values for **6-X**, which varied by only 0.28 V.

Clearly, while the concept of electrocatalytic CH bond activation according to Fig. 1. remains apparent, a system possessing higher oxidation potentials and greater stability of the oxidation product is needed for fruition. The more common cycle for Fig. 1 involves the $\text{p}K_{\text{a}}$ of L_nMXH and the E_{ox}^0 of L_nMX^- , but in this study the compounds were chosen as hydroquinone mimics, hence the $\text{p}K_{\text{a}}$ of L_nMXH^+ should be <0 , i.e., dissociation should occur spontaneously upon oxidation. Since the 1.36 $\text{p}K_{\text{a}}$ factor is rather modest, this was not considered to be a serious detriment to the proposed CH bond activation, but it certainly could be a source of overestimation in terms of limiting the strength of the bonds potentially activated if the $\text{p}K_{\text{a}}$ is much less than zero. For another view of this point, consider the more conventional way of estimating the OH bond strength of $(p\text{-XC}_6\text{H}_4\text{O})_5\text{W}(\text{O-C}_6\text{H}_4\text{OH})$ (**6-X**). First, the $\text{p}K_{\text{a}}$ of **6-X** would be determined (e.g., the $\text{p}K_{\text{a}}$ of **6-X** would be >0), then the oxidation potential of $(p\text{-XC}_6\text{H}_4\text{O})_5\text{W}(\text{OC}_6\text{H}_4\text{O}^-)$ would be measured. It is likely that the oxidation potential for this anionic species would be far less positive than for **6-X**, thereby compensating for the $\text{p}K_{\text{a}}$ increase. Unfortunately, attempts to generate a stable anion of **6-X** via deprotonation failed, and mild bases afforded H-bonded coordination networks [33]. It is likely that $(p\text{-XC}_6\text{H}_4\text{O})_5\text{W}(\text{O-C}_6\text{H}_4\text{O}^-)$, which could also be considered as $[(p\text{-XC}_6\text{H}_4\text{O})_5\text{W}^{\text{IV}}(\text{OC}_6\text{H}_4\text{O})]^-$, is an unstable species.

4. Experimental

4.1. General considerations

All manipulations were performed using either glovebox or high vacuum line techniques. Hydrocarbon solvents containing 1–2 mL of added tetraglyme, and ethereal solvents were distilled under nitrogen from purple sodium benzophenone ketyl and vacuum transferred from same prior to use. C_6D_6 and acetonitrile were dried over activated 4 Å molecular sieves, vacuum transferred and stored under N_2 . All other chemicals were purchased from commercial sources and used as received. All glassware was oven dried, and NMR tubes for sealed tube experiments were additionally flame-dried under dynamic vacuum. All phenols were purchased from Aldrich Chem. Co. and recrystallized prior to use.

NMR spectra were obtained using INOVA-400 and Unity-500 spectrometers, and chemical shifts are reported relative to C_6D_6 (^1H , 7.15; $^{13}\text{C}\{^1\text{H}\}$, 128.39) or acetone- d_6 (^1H , 2.05; $^{13}\text{C}\{^1\text{H}\}$, 29.92). Infrared spectra were recorded on a Nicolet Impact 410 spectrophotometer interfaced to a Gateway PC. Elemental analyses were performed by Oneida Research Services, Whitesboro, NY, or Robertson Microtit Laboratories, Madison, NJ. Magnetic moments were determined in C_6D_6 or thf-d_8 at room temperature using Evans method with an applied diamagnetic correction.

4.2. Procedures

4.2.1. $(p\text{-PhCH}_2\text{OC}_6\text{H}_4\text{O})_6\text{W}$ (**1-OCH₂Ph**)

$\text{W}(\text{OCH}_3)_6$ (1.150 g, 3.11 mmol) and 4-benzyloxyphenol (5.00 g, 25.0 mmol) were combined in a large glass bomb with 40 mL toluene. The bomb was lowered into a salt bath until the solvent level was covered and the temperature settled at 173°C. After 24 h, the reaction was judged incomplete by a TLC using toluene as the eluting solvent. $\text{W}(\text{OC}_6\text{H}_4\text{OCH}_2\text{C}_6\text{H}_5)_6$ has an R_f of 0.70 while the R_f of $\text{W}(\text{OC}_6\text{H}_4\text{OCH}_2\text{C}_6\text{H}_5)_5(\text{OCH}_3)$ is 0.65 and other less substituted products have lower R_f s. The temperature was gradually increased, until after 24 h at 213 °C the reaction was complete except for a trace of a lower R_f spot. Toluene was added to the reaction mixture and it was washed with 3×350 mL 5% NaOH (aq). The deep red solution was dried over Na_2SO_4 and the solvent stripped on a rotary evaporator. The resulting dark red, very viscous oil was placed under high vacuum for several hours. ^1H NMR showed clean **1-OCH₂Ph** and toluene. The yield of 4.41 g translates to 3.89 g **1-OCH₂Ph** when the presence of toluene was accounted for, giving an actual yield of 91%.

4.2.2. $(p\text{-HOC}_6\text{H}_4\text{O})_6\text{W}$ (**1-OH**)

1-OCH₂Ph (3.85 g, 2.79 mmol) was dissolved in 125 mL toluene/125 mL ethanol along with 500 mg 10% PdC. The

mixture was stirred under 1 atm H₂ and checked periodically by TLC using 100% ethyl acetate as the eluting solvent. Incompletely deprotected products have higher R_fs (0.85 or greater) than the final product (R_f = 0.80). After 4 h, the reaction was mostly complete, but required 24 h until only a trace spot at R_f = 0.85 remained. The reaction mixture was filtered through celite and the celite washed with ethanol. Volatiles were removed on a rotary evaporator and the product transferred to a 100 mL flask with THF. The THF was stripped and dry THF was added and removed. Dry THF was added and then stripped twice more to remove traces of water. The product was crystallized from 50 mL benzene/3–4 mL THF and dried under vacuum for 12 h (1.778 g, 60% based on (p-HOC₆H₄O)₆·W·2THF·C₆H₆) (1-OH·2THF·C₆H₆). ¹H NMR in acetone-d₆ indicated pure 1-OH with 2.0 equivalents of THF and 0.9 equivalents of benzene. Elemental analysis indicated some loss of solvent before combustion: *Anal.* Calc. for W(OC₆H₄OH)₆·1.5 THF: C, 53.29; H, 4.47. Found: C, 53.11; H, 4.55%.

4.2.3. General (p-XC₆H₄O)₆W (1-X, X = H, CH₃, OCH₃, Cl, Br)

To a 250 mL flask attached to a reflux condenser was added WCl₆ (5 g, 12.6 mmol). A sidearm flask containing p-XC₆H₄OH (81.7 mmol) was connected to the flask, which was attached to an argon line equipped with a bubbler. 100 mL of chlorobenzene was added and the phenol was gradually tapped into the flask and HCl (g) was evolved. The solution was refluxed for 12–24 h followed by an argon purge to remove residual HCl (g). The solution was washed twice with 10% NaOH (aq) and deionized water, then dried over MgSO₄. The solvent was removed under reduced pressure, and the product crystallized from petroleum ether (X = Me, Cl, Br) or ethanol (X = OMe, H).

(a) (p-MeOC₆H₄O)₆W (1-CH₃). TLC (50% ethyl acetate:hexane): R_f = 0.59. ¹H NMR (acetone-d₆): δ 3.72 (s, Me), 6.78 (d, J = 9 Hz, CH), 6.85 (d, J = 9 Hz, CH). ¹³C{¹H} NMR (acetone-d₆): δ 55.85 (Me), 114.67 (C_m), 121.91 (C_o), 156.71 (C_p), 156.93 (C_{ipso}).

(b) (p-MeC₆H₄O)₆W (1-CH₃). TLC (25% ethyl acetate:hexane): R_f = 0.66. ¹H NMR (acetone-d₆): δ 2.33 (s, Me), 6.83 (d, J = 9 Hz, CH), 7.05 (d, J = 9 Hz, CH). ¹³C{¹H} NMR (acetone-d₆): δ 20.69 (Me), 120.96 (C_o), 130.17 (C_m), 133.77 (C_p), 160.78 (C_{ipso}).

(c) (p-ClC₆H₄O)₆W (1-Cl). TLC (25% ethyl acetate:hexane): R_f = 0.73. ¹H NMR (acetone-d₆): δ 7.01 (d, J = 9 Hz, CH), 7.32 (d, J = 9 Hz, CH). ¹³C{¹H} NMR (acetone-d₆): δ 122.63 (C_o), 129.81 (C_p), 130.04 (C_m), 160.79 (C_{ipso}).

(d) (p-BrC₆H₄O)₆W (1-Br). TLC (15% ethyl acetate:hexane): R_f = 0.68. ¹H NMR (acetone-d₆): δ 6.96 (d, J = 9 Hz, CH), 7.47 (d, J = 9 Hz, CH). ¹³C{¹H} NMR (acetone-d₆): δ 123.07 (C_o), 133.07 (C_m), 161.24 (C_{ipso}), C_p obscured.

(e) (C₆H₅O)₆W (1-H). TLC (25% ethyl acetate:hexane): R_f = 0.60. ¹H NMR (acetone-d₆): δ 6.90 (t, J = 8 Hz, CH_p), 6.96 (d, J = 8 Hz, CH), 7.27 (t, J = 8 Hz, CH_m). ¹³C{¹H} NMR (acetone-d₆): δ 121.16 (C_o), 124.59 (C_p), 129.81 (C_p), 129.88 (C_m), 162.69 (C_{ipso}).

4.2.4. General (p-XC₆H₄O)₅W(OC₆H₄OH) (6-X, X = OMe, Me, H, Cl, Br)

A 250 mL round bottom flask was charged with 1-X (5.4 mmol), 4-(benzyloxy)phenol (10 mmol), p-toluenesulfonic acid monohydrate (1.1 mmol), and chlorobenzene (100 mL). The solution was refluxed under an argon atmosphere for 1–3 h and the reaction was monitored by TLC (silica plate) for optimization of the mono-substituted product (p-XC₆H₄O)₅W(OC₆H₄OCH₂Ph) (5-X). Toluene (100 mL) was added to reaction solution and the mixture was washed three times with both 5% NaOH(aq) and de-ionized water. It was dried over MgSO₄, and the solvent was removed under reduced pressure. The resulting red oil was dissolved in a mixture of toluene (50 mL) and absolute ethanol (50 mL) followed by an argon purge. 10% Palladium on carbon (0.125 g) was added and the heterogeneous solution was stirred under hydrogen (1 atm) for 5 h. Analysis by TLC of the hydrogenated solution versus the starting solution indicated complete hydrogenation. The catalyst was removed by filtration and the volatiles were removed on a rotary evaporator. Purification was accomplished by column chromatography on silica using an appropriate mixture of ethyl acetate and hexane as the mobile phase. Further purification by recrystallization from methanol was performed when possible.

(a) (p-MeOC₆H₄O)₅W(O-C₆H₄OH) (6-OMe). TLC(50% ethyl acetate:hexane): R_f = 0.50. ¹H NMR (acetone-d₆): δ 3.73 (s, 15H, Me), 6.71 (d, J = 9 Hz, 2H, H'_o or H'_m), 6.80 (m, 12H, H_m and C'H'_o or C'H'_m), 6.86 (m, 10H, CH_o), 8.20 (s, 1H, OH). ¹³C{¹H} NMR (acetone-d₆): 55.83 (Me), 114.63 (C_m), 115.98 (C'_m), 121.90 (C_o), 122.02 (C'_o), 154.43 (C'_p), 156.25 (C'_{ipso}), 156.60 (C_p), 156.98 (C_{ipso}). *Anal.* Calc for C₄₁H₄₀O₁₂W: C, 54.2; H, 4.5. Found: C, 54.2; H, 4.4%.

(b) (p-MeC₆H₄O)₅W(OC₆H₄OH) (6-Me). TLC (25% ethyl acetate:hexane): R_f(5-Me) = 0.44; R_f(6-Me) = 0.18. ¹H NMR (acetone-d₆): δ 2.32 (s, 15H, Me), 6.71 (d, J = 9 Hz, 2H, C'H'_o or C'H'_m), 6.82 (m, 12H, H_o and H'_o or H'_m), 7.05 (d, J = 9 Hz, 10H, H_m), 8.31 (s, 1H, OH). ¹³C{¹H} NMR (acetone-d₆): 20.86 (Me), 115.93 (C'_m), 120.92 (C_o), 122.20 (C'_o), 130.16 (C_m), 133.57 (C_p), 154.81 (C'_p), 156.13 (C'_{ipso}), 160.85 (C_{ipso}). *Anal.* Calc for C₄₁H₄₀O₇W: C, 59.4; H, 4.9. Found: C, 59.5; H, 4.8%.

(c) (p-BrC₆H₄O)₅W(OC₆H₄OH) (6-Br). TLC (3% ethyl acetate:hexane): R_f(5-Br) = 0.75; R_f(6-Br) = 0.44. ¹H NMR (acetone-d₆): δ 6.71 (m, 2H, C'H'_o or C'H'_m), 6.94 (m, 12H, H_o and C'H'_o or C'H'_m), 7.46 (m, 10H, H_m), 8.62 (s, 1H, OH).

(d) $(p\text{-ClC}_6\text{H}_4\text{O})_5\text{W}(\text{OC}_6\text{H}_4\text{OH})$ (**6-Cl**). TLC (3% ethyl acetate:hexane): $R_f(\mathbf{5-Cl}) = 0.70$; $R_f(\mathbf{6-Cl}) = 0.41$. 4-Chlorophenol could not be separated from **6-Cl** by column chromatography or crystallization and impeded definitive spectroscopic characterization.

(e) $(\text{C}_6\text{H}_5\text{O})_5\text{W}(\text{OC}_6\text{H}_4\text{OH})$ (**6-H**). TLC (25% ethyl acetate:heptane): $R_f(\mathbf{5-H}) = 0.48$; $R_f(\mathbf{6-H}) = 0.25$. ^1H NMR (acetone- d_6): δ 6.72 (d, $J = 8$ Hz, 2H, $\text{C}'\text{H}'_o$ or $\text{C}'\text{H}'_m$), 6.93 (m, 17H, CH_o , CH_m and $\text{C}'\text{H}'_o$ or $\text{C}'\text{H}'_m$), 7.26 (m, 10H, d), 8.32 (s, 1H, OH). $^{13}\text{C}\{^1\text{H}\}$ NMR (acetone- d_6): 115.99 (C'_m), 121.09 (C'_o), 122.30 (C'_o), 124.31 (C'_p), 129.83 (C'_m), 154.31 (C'_p), 155.94 (C'_{ipso}), 162.81 (C'_{ipso}).

4.2.5. $\{K[(p\text{-ClC}_6\text{H}_4\text{O})_6\text{W}]\}_\infty$ (**8-Cl**)

A 25 mL round bottom flask was charged with **1-Cl** (0.300 g, 0.316 mmol), Raney Nickel (0.075 g, 1.28 mmol), diethyl ether (15 mL), and ethanol (0.40 mL). Potassium metal (0.02 g, 0.5 mmol) was added and the purple-red solution was stirred for 2 h. The resulting heterogeneous orange solution was filtered, and the filtrate layered with pentane yielding the product as orange crystals (0.191 g, 61%). *Anal. Calc.* for $\text{C}_{36}\text{H}_{24}\text{O}_6\text{Cl}_6\text{KW}$: C, 43.8; H, 2.5; Cl, 21.5. Found: C, 44.0; H, 2.5; Cl, 20.6%.

4.2.6. $\{K[(\text{C}_6\text{H}_5\text{O})_6\text{W}]\}_\infty$ (**8-H**)

A 25 mL round bottom flask was charged with **1-H** (0.200 g, 0.269 mmol), Raney Nickel (0.050 g, 0.852 mmol), diethyl ether (10 mL), and ethanol (0.30 mL). Potassium metal (0.02 g, 0.5 mmol) was added and the purple-red solution was stirred for 2 h resulting in a yellow precipitate and light yellow solution. The solid was collected by filtration and separated from the remaining Raney Nickel by dissolution in minimal THF followed by filtration and crystallization by slow evaporation (0.093 g, 44%). ^1H NMR (thf- d_8): δ 4.96 ($\nu_{1/2} \sim 20$ Hz, 6H, H_p), 6.63 ($\nu_{1/2} \sim 40$ Hz, 12H, CH), 9.28 ($\nu_{1/2} \sim 20$ Hz, 12H, CH). The ^1H NMR spectrum is similar to that obtained by Wilkinson and coworkers [45] (acetone- d_6) for an independent synthesis of $\text{KW}(\text{OPh})_6$. $\mu_{\text{eff}}(293\text{K}) = 1.5 \mu_{\text{B}}$ (Evans' method in thf- d_8).

4.2.7. Preparation of $[(p\text{-ClC}_6\text{H}_4\text{O})_6\text{W}][\text{K}(\text{PhCN})_4]$ (**9-Cl**)

A 10 mm O.D. glass tube was charged with **8-Cl** (0.081 g, mmol) and benzonitrile (4 mL). The solution was degassed, sealed, and heated at 100 °C for 5 d with no color change. The product was isolated as an orange solid (0.072 g, 63%) after solvent removal followed by trituration with pentane. ^1H NMR (thf- d_8): δ 7.12 ($\nu_{1/2} \sim 160$ Hz, 12H, CH), 7.51 (t, $J = 8$ Hz, 8H, PhCN H_p or H_m), 7.63 (t, $J = 8$ Hz, 4H, PhCN H_p or H_m), 7.69 (d, $J = 8$ Hz, 8H, PhCN H_o), 9.18 ($\nu_{1/2} \sim 10$ Hz, 12H, CH).

4.2.8. Electrochemistry: general procedure

The working electrode was a 1 mm diameter platinum disk electrode sealed in glass. In cases where fast sweep rates were employed, a 75 μm platinum disk electrode, sealed in glass, was used. All measurements were carried out inside a glove-box (Vac. Atmospheres) at 25 °C. Acetonitrile (Burdick & Jackson; distilled in glass) and dried over 4 Å molecular sieves was used as the solvent. Tetra-*n*-butyl ammonium hexafluorophosphate (TBAG; G.F. Smith) used as supporting electrolyte was recrystallized 3× from absolute ethanol and dried under vacuum for 96 h. A Princeton Applied Research Model 173 Potentiostat with a model 175 Programmer were used. Data at sweep rates at or below 500 mV/s were recorded on a Soltec X–Y recorder. At faster sweep rates, data were recorded on a Tektronix digital storage oscilloscope. A background scan of solvent and supporting electrolyte out to the potential limits of the experiment, was always varied out. A sweep rate dependence of the peak current was carried out for all the materials involved and in all cases the current was proportional to the square root of the sweep rate (over a typical range of 50–1000 mV/s) as anticipated for a diffusion controlled process. A silver wire was employed in order to ensure rigorous exclusion of water, especially since experiments were done inside a dry box. Reproducibility of the peak potentials – even those that are irreversible – was roughly ± 10 –15 mV.

4.2.9. X-ray crystal structure determination: $\{K[(p\text{-ClC}_6\text{H}_4\text{O})_6\text{W}]\}_\infty$ (**8-Cl**)

X-ray diffraction quality single crystals were obtained by layering a saturated diethyl ether solution of **8-Cl** with pentane. One orange crystal (0.3 × 0.15 × 0.1 mm) was selected, coated in polyisobutylene, and placed under a 173 K nitrogen stream on the goniometer head of a Siemens SMART CCD Area Detector system equipped with a fine-focus molybdenum X-ray tube ($\lambda = 0.71073 \text{ \AA}$). Preliminary diffraction data revealed a triclinic crystal system. A hemisphere routine was used for data collection. The data was subsequently processed with the Bruker SAINT program and the space group was determined to be $P\bar{1}$. The data was corrected for absorption with SADABS, solved by direct methods, completed by subsequent difference Fourier syntheses and refined by full-matrix least-squares procedures (SHELXTL). All non-hydrogen atoms were refined with anisotropic displacement parameters and hydrogen atoms were included at calculated positions.¹

¹ Cambridge Crystallographic Data Centre deposition number: CCDC 247677.

Acknowledgements

The National Science Foundation and the Department of Chemistry and Chemical Biology at Cornell University are gratefully acknowledged for support. T.P.V. thanks the NSF for an Inorganic Materials Traineeship. We thank a referee for pointing out the work of Cheng, Handoo, Xue and Parker [50].

References

- [1] J.A. Labinger, J.E. Bercaw, *Nature* 417 (2002) 506–514.
- [2] S. Stahl, J.A. Labinger, J.E. Bercaw, *Angew. Chem. Int. Ed. Engl.* 37 (1998) 2180–2192.
- [3] (a) A.E. Shilov, G.B. Shul'pin, *Activation and Catalytic Reactions of Saturated Hydrocarbons in the Presence of Metal Complexes*, Kluwer Academic Press, Dordrecht, Netherlands, 2000; (b) A.E. Shilov, A.A. Shteinmann, *Coord. Chem. Rev.* 24 (1977) 97–143.
- [4] M.S. Freund, J.A. Labinger, N.S. Lewis, J.E. Bercaw, *J. Mol. Catal.* 87 (1994) L11–L16.
- [5] M. Lin, C. Shen, E.A. Garcia-Zayas, A. Sen, *J. Am. Chem. Soc.* 123 (2001) 1000–1001.
- [6] R.A. Periana, O. Mironov, D. Taube, G. Bhalla, C.J. Jones, *Science* 301 (2003) 814–818.
- [7] R.A. Periana, D.J. Taube, S. Gamble, H. Taube, T. Satoh, H. Fujii, *Science* 280 (1998) 560–564.
- [8] R.F. Jordan, D.F. Taylor, N.C. Baenziger, *Organometallics* 9 (1990) 1546–1557.
- [9] C.G. Jia, D.G. Piao, J.Z. Oyamada, W.J. Lu, T. Kitamura, Y. Fujiwara, *Science* 287 (2000) 1992–1995.
- [10] T. Matsumoto, R.A. Periana, D.J. Taube, H. Yoshida, *J. Mol. Catal. A: Chem.* 180 (2002) 1–18.
- [11] (a) K.M. Waltz, J.F. Hartwig, *J. Am. Chem. Soc.* 122 (2000) 11358–11369; (b) H.Y. Chen, S. Schlecht, T.C. Temple, J.F. Hartwig, *Science* 287 (2000) 1995–1997; (c) C.E. Webster, Y.B. Fan, M.B. Hall, D. Kunz, J.F. Hartwig, *J. Am. Chem. Soc.* 125 (2003) 858–859.
- [12] (a) R.E. Maleczka, F. Shi, D. Holmes, M.R. Smith, *J. Am. Chem. Soc.* 125 (2003) 7792–7793; (b) J.Y. Cho, M.K. Tse, D. Holmes, R.E. Maleczka, M.R. Smith, *Science* 295 (2002) 305–308.
- [13] C.M. Jensen, *Chem. Commun.* (1999) 2443–2449.
- [14] (a) K.B. Renkema, Y.V. Kissin, A.S. Goldman, *J. Am. Chem. Soc.* 125 (2003) 7770–7771; (b) K. Krogh-Jespersen, M. Czerw, N. Summa, K.B. Renkema, P.D. Achord, A.S. Goldman, *J. Am. Chem. Soc.* 124 (2002) 11404–11416.
- [15] G.W. Parshall, S.D. Ittel, *Homogeneous Catalysis: The Applications and Chemistry of Catalysis by Soluble Transition Metal Complexes*, 2nd ed., Wiley, New York, 1992.
- [16] R.A. Sheldon, J.K. Kochi, *Metal-catalyzed Oxidations of Organic Compounds*, Academic Press, New York, 1981.
- [17] W.D. Jones, E.T. Hessell, *J. Am. Chem. Soc.* 115 (1993) 554–562.
- [18] (a) P.O. Stoutland, R.G. Bergman, S.P. Nolan, C.D. Hoff, *Polyhedron* 7 (1988) 1429–1440; (b) R.A. Periana, R.G. Bergman, *J. Am. Chem. Soc.* 108 (1986) 7332–7346.
- [19] (a) J.L. Bennett, P.T. Wolczanski, *J. Am. Chem. Soc.* 119 (1997) 10696–10719; (b) J.L. Bennett, T.P. Vaid, P.T. Wolczanski, *Inorg. Chim. Acta* 270 (1998) 414–423.
- [20] M.L.H. Green, P.J. Knowles, *J. Chem. Soc., Chem. Commun.* (1970) 1677.
- [21] E.A. Ambundo, R.A. Friesner, S.J. Lippard, *J. Am. Chem. Soc.* 124 (2002) 8770–8771, and references therein.
- [22] M. Newcomb, R. Shen, Y. Lu, M.J. Coon, P.F. Hollenberg, D.A. Kopp, S.J. Lippard, *J. Am. Chem. Soc.* 124 (2002) 6879–6886, and references therein.
- [23] (a) P. Chaudhuri, M. Hess, U. Flörke, K. Wieghardt, *Angew. Chem. Int. Ed.* 37 (1998) 2217–2220; (b) P. Chaudhuri, M. Hess, J. Muller, K. Hildenbrand, E. Bill, T. Weyhermüller, K. Wieghardt, *J. Am. Chem. Soc.* 121 (1999) 9599–9610.
- [24] (a) R.C. Pratt, T.D.P. Stack, *J. Am. Chem. Soc.* 125 (2003) 8716–8717; (b) Y.D. Wang, J.L. DuBois, B. Hedman, K.O. Hodgson, T.D.P. Stack, *Science* 279 (1998) 537–540.
- [25] C.R. Goldsmith, R.T. Jonas, T.D.P. Stack, *J. Am. Chem. Soc.* 124 (2002) 83–96.
- [26] (a) J.-U. Rohde, J.-H. In, M.H. Lim, W.W. Brennessel, M.R. Bukowski, A. Stubna, E. Münck, W. Nam, L. Que Jr., *Science* 299 (2003) 1037–1039; (b) M.H. Lim, J.-U. Rohde, A. Stubna, M.R. Bukowski, M. Costas, R.Y.N. Ho, E. Münck, W. Nam, L. Que Jr., *Proc. Natl. Acad. Sci.* 100 (2003) 3665–3670.
- [27] J. Kaizer, E.J. Klinker, N.Y. Oh, J.-U. Rohde, W.J. Song, A. Stubna, J. Kim, E. Münck, W. Nam, L. Que Jr., *J. Am. Chem. Soc.* 126 (2004) 472–473.
- [28] (a) D.D.M. Wayner, V.D. Parker, *Acc. Chem. Res.* 26 (1993) 287–294; (b) M. Tilset, V.D. Parker, *J. Am. Chem. Soc.* 111 (1989) 6711–6717; M. Tilset, V.D. Parker, *J. Am. Chem. Soc.* 112 (1990) 2843; (c) V.D. Parker, K.L. Handoo, F. Roness, M. Tilset, *J. Am. Chem. Soc.* 113 (1991) 7493–7498.
- [29] J.M. Mayer, *Acc. Chem. Res.* 31 (1998) 441–450.
- [30] K.A. Gardner, J.M. Mayer, *Science* 269 (1995) 1849–1851.
- [31] (a) K. Wang, J.M. Mayer, *J. Am. Chem. Soc.* 119 (1997) 1470–1471; (b) J.R. Bryant, J.M. Mayer, *J. Am. Chem. Soc.* 125 (2003) 10351–10361, and references therein.
- [32] L.B. Handy, K.G. Sharp, F.E. Brinckman, *Inorg. Chem.* 11 (1972) 523–531.
- [33] T.P. Vaid, O.L. Sydora, R.E. Douthwaite, P.T. Wolczanski, E.B. Lobkovsky, *J. Chem. Soc. Chem. Commun.* (2001) 1300–1301.
- [34] S.M. Beshouri, I.P. Rothwell, *Inorg. Chem.* 25 (1986) 1962–1964.
- [35] H. von Funk, W. Baumann, *Z. anorg. Chem.* 231 (1937) 264–268.
- [36] P.I. Mortimer, M.I. Strong, *Aust. J. Chem.* 18 (1965) 1579–1587.
- [37] B.R. Eggins, J.Q. Chambers, *J. Electrochem. Soc.* 117 (1970) 186–192.
- [38] M.W. Lehmann, D.H. Evans, *J. Electroanal. Chem.* 500 (2001) 12–20, and references therein.
- [39] L. Papouchado, R.W. Sandford, G. Petrie, R.N. Adams, *J. Electroanal. Chem.* 65 (1975) 275–284.
- [40] C. Iwakura, M. Tsunaga, H. Tamura, *Electrochem. Acta* 17 (1972) 1391–1400.
- [41] D.T.Y. Yiu, M.F.W. Lee, W.W.Y. Lam, T.-C. Lau, *Inorg. Chem.* 42 (2003) 1225–1232.
- [42] J.A. Richards, D.H. Evans, *J. Electroanal. Chem.* 81 (1977) 171–187.
- [43] J. Berkowitz, G.B. Ellison, D. Gutman, *J. Phys. Chem.* 98 (1994) 2744–2765, and references therein.
- [44] D.E. Berning, B.C. Noll, D.L. DuBois, *J. Am. Chem. Soc.* 121 (1999) 11432–11447.
- [45] H. Funk, H. Matschiner, H. Naumann, *Z. Anorg. Allg. Chem.* 340 (1965) 75–81.
- [46] J.I. Davies, J.F. Gibson, A.C. Skapski, G. Wilkinson, W.-K. Wong, *Polyhedron* 1 (1982) 641.
- [47] (a) M.L. Listemann, J.C. Dewan, R.R. Schrock, *J. Am. Chem. Soc.* 107 (1985) 7207–7208; (b) M.A. Lockwood, P.E. Fanwick, O. Eisenstein, I.P. Rothwell, *J. Am. Chem. Soc.* 118 (1996) 2762–2763.

- [48] (a) J.K. Kochi (Ed.), *Free Radicals*, Wiley, New York, 1973;
(b) J.H. Knox, in: Z.B. Alfassi (Ed.), *Chemical Kinetics of Small Organic Radicals*, CRC Press, Boca Raton, FL, 1988.
- [49] L.M. Slaughter, P.T. Wolczanski, T.R. Klinckman, T.R. Cundari, *J. Am. Chem. Soc.* 122 (2000) 7953–7975.
- [50] J.-P. Cheng, K.L. Handoo, J. Xue, V.D. Parker, *J. Org. Chem.* 58 (1993) 5050–5054.